Cellulose Acetate Nanocomposite Membranes for Water Desalination Applications

A. R. Ramadan*, A.M.K. Esawi**, N. El-Badawi***
and M. Mahmoud *****

*Department of Chemistry, The American University in Cairo,
AUC Avenue, New Cairo 11835, Egypt, aramadan@aucegypt.edu
**Department of Mechanical Engineering, The American University in Cairo,
AUC Avenue, New Cairo 11835, Egypt, a_esawi@aucegypt.edu
***Department of Chemistry, The American University in Cairo,
AUC Avenue, New Cairo 11835, Egypt, nony@aucegypt.edu
****Department of Chemistry, The American University in Cairo,
AUC Avenue, New Cairo 11835, Egypt, 3m@aucegypt.edu

ABSTRACT

Cellulose acetate (CA) membranes incorporating on the one hand functionalized carbon nanotubes (CNTs) and on the other graphene oxide (GOX) as nanofillers were prepared by phase inversion. Scanning electron microscopy (SEM) indicated that both types of nanofillers were well dispersed in the membrane polymer matrix with no evidence of agglomerations. Nitrogen adsorption studies indicated that membrane porosity decreased with the presence of nanofillers, leading to lower surface area values. However this decrease in porosity was significantly less pronounced for GOX nanocomposite membranes than CNT nanocomposite membranes. In spite of this, CNT membranes showed lower permeation rates with significantly higher salt rejection values. This seems to indicate that the interfacial region between nanofiller and the polymer matrix plays a role in membrane performance, affected by the interactions between filler and matrix.

Keywords cellulose acetate, carbon nanotubes, graphene, membranes, desalination

1 INTRODUCTION

The role of membrane technology in water desalination has been on the rise over the past decade with more than 50% of global fresh water production resulting from membrane technology [1]. Different membrane prepartion conditions and additives are used to enhance membrane performance. Graphene-based nanofillers [2, 3] and CNTs [4, 5] have received recent attention in this regard. Their abilities to enhance membranes hydrophilicity, as well as change membrane porosity can significantly enhance membrane performance [2-5]. Though the mechanism of water transport through graphene based nanofillers is not yet well understood, molecular dynamics simulations attribute the ultra fast water transport behavior to the almost frictionless flow of water between graphene sheets, whether they are layered or as nanotubes [6, 7]. The current work aims at understanding the role of GOX and functionzlized CNTs in enhancing the performance of CA membranes for water desalination applications.

2 EXPERIMENTAL

CNTs (Baytubes® C150P, C-purity ≥95 wt.%) were functionalized as described elsewhere [8], with the aim of improving their interaction with the polymer matrix. The functionalized CNTs, and GOX (ACS Material, purity ~99%, single layer ratio ~99%, thickness ~0.8 to 1.2 nm) were each added to 17 wt% CA (average molecular weight of 50,000 Da, and 39.7 wt.% acetyl content, Sigma Aldrich) solution in acetone (Sigma Aldrich, purity ≥99.8%) with 20 wt% of deinoized water, a non-solvent to CA. The nanotubes and GOX were each first dispersed in deionized water by sonication for 10 s, then added gradually to the CA solution with vigorous stirring, followed by sonication for 2 min, and resting of each of the mixtures for 18 h in order to allow any air bubbles in the solution to dissipate. Different masses of the CNTs and the GOX were used to obtain polymer-CNTs and polymer-GOX mixtures of 0.001 and 0.002 wt% of nanofiller. A blank CA solution devoid of CNTs and GOX was also prepared. Each of these solutions was cast on a glass substrate, using a casting knife, then directly immersed in a deionized water bath kept at room temperature for phase inversion to take place by solvent/non-solvent demixing. The final thickness of all membranes was 100 ± 10 μm. The process resulted in the nanocompoiste membranes 1CNT, 2CNT, 1GOX, 2GOX, and the blank membrane CABlank.

Membrane characterization was conducted with a Leo Supra 55 field emission scanning electron microscope (FESEM), and membrane porosity determined by N_2 adsorption at 77 K using an ASAP 2020-Micromeretics apparatus. For water permeation and salt rejection, a 5 cm diameter membrane disk was placed in a test cell (Sterlitech HP4750 stirred cell), which was filled with a 5000 ppm $MgSO_4$ (Sigma Aldrich, purity ≥ 99.5%) feed solution. A pressure of 24 bars was applied using N_2 gas. Permeation

rate was calculated using Equation (1), where J is the permeation rate in L/m^{2}h, V is the permeate volume, A is the membrane area on which pressure is applied, and t is the time.

$$J = V/(A\ t) \quad (1)$$

Salt rejection R (%) was calculated using equation (2), where C_p is the salt concentration (in ppm) of the permeate and C_f, the salt concentration of the feed (in ppm).

$$R = 100\ (1 - (C_p/C_f)) \quad (2)$$

Permeation and salt rejection was determined in triplicate for each of the five membrane samples, and the average values reported.

3 RESULTS

3.1 Porosity

Figures 1 and 2 present the differential pore volume and pore surface area for the five membrane samples. Pores larger than 10 nm in diamter accounted for most of the pore volume for all membranes. Pores smaller than 10 nm in diameter accounted for limited differential pore volumes, with distinct values at pore diameters of 1.7 and 2.7 nm (inset in Figure 1). These pores, however, significantly accounted for pore surface areas, denoting their large numbers in the membrane samples.

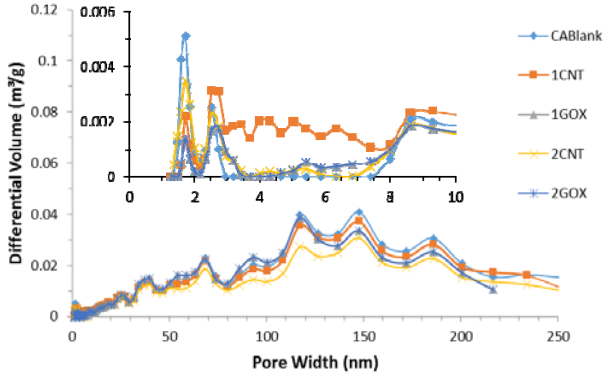

Figure 1. Differential pore volume vs. pore width for the different membranes.

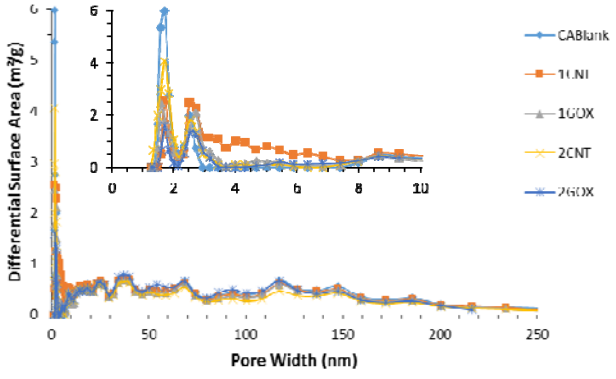

Figure 2. Differential pore surface area vs. pore width for the different membranes.

Generally, the presence of the nanofillers led to the decrease in membrane porosity. However, this decrease was not the same for the two types of nanofillers, neither was it the same for different values of pore widths. Though the decrease in overall porosity was more significant for the 2CNT membrane, this membrane exhibited the highest values for pore differential volume and surface area for the four nanocomposite membranes prepared, i.e. a focus of membrane porosity occurred at the smaller pore diamter of 1.7 nm. Membrane sample 2CNT behaved somewhat differently, with smaller values for differential pore volume and surface area at the pore diamter of 1.7 nm, but higher values at the pore diamter of 2.7 nm, and more generally at pore diamters of up to 10 nm. Membranes 1GOX and 2GOX exhibited porosity trends similar to each other. Differetial pore volume and surface area values were similar and significantly smaller than CABlank, as well as 1CNT and 2CNT at pore widths of 1.7 nm and 2.7 nm. The above is reflected in the values of membrane surface areas presented in Table 1.

3.2 Morphology

FESEM images showed that all membranes exhibited macrovoid formations, surrounded by a porous membrane structure, with a dense layer. The thickness of the dense layer appeared to be the same in all membarnes. Representative FESEM images are included in Figure 3.

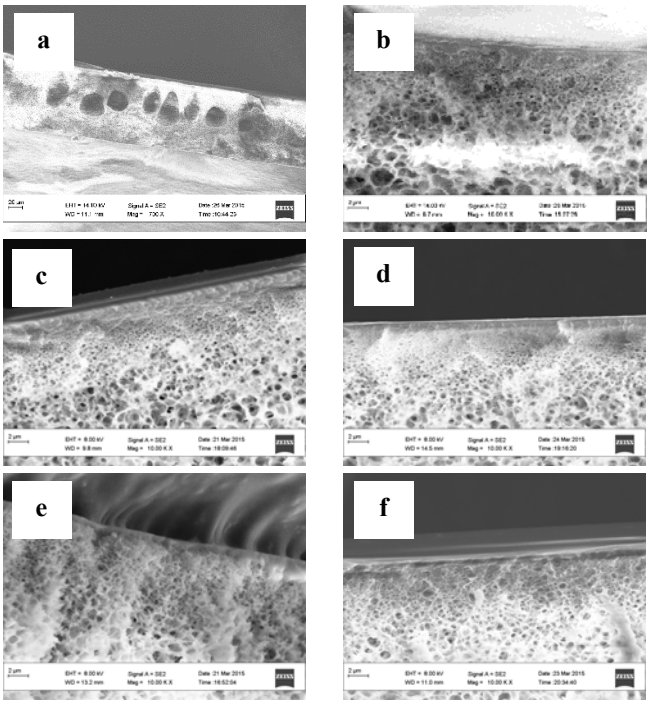

Figure 3. Representative FESEM images: (a) CABlank showing the microvoid structures typical of all prepared membranes, (b)-(f) membrane porosity with the dense layer for CABlank, 1CNT, 2CNT, 1GOX, 2GOX respectively.

	Surface Area (m^2/g)	Permeation Rate ($L/m^2.h$)	Salt Rejection (%)
CABlank	5.7	13.2	72
1CNT	4.7	6.5	91
2CNT	5.2	5.5	94
1GOX	5.4	8.2	84
2GOX	4.0	8.7	78

Table 1. Surface area values, permeation rates and salt rejection values for the different membrane samples prepared

It is important to note that none of the nanocomposite membranes showed any visible agglomerations of the nanofillers used (either CNTs or GOX), denoting the success of the prepartion process followed in leading to a good dispersion of the nanofiller used within the CA matrix.

3.3 Permeation and salt rejection

Table 1 presents values for membrane water permeation and salt rejection. The presence of nanofillers significantly inproved salt rejection with a reduction in permeation rates, corroborated by the reduction of the overall membrane porosity, as reflected by the decrease in membrane surface area values. Membrane porosity seems to indicate a significant role of the smaller pores (< 6 nm) in salt rejection.

The different nanofiller types used had different effects on permeation and salt rejection. For the case of CNTs, the permeation rate decreased with the increase in CNT content, with an associated increase in salt rejection. On the other hand, for GOX, the permeation rate increased with GOX content, with an associated decrease in salt rejection. This difference might be due to the different interactions between each type of nanofiller and the polymer matrix, affecting the interfacial region between them, which seems to be playing a role in permeation and salt rejection.

4 CONCLUSIONS

Nanocomposite CA membranes, prepared by phase inversion, exhibited a good dispersion of the two different types of nanofillers used: functionalized CNTs, and GOX.

The presence of the nanofillers led to an overall decrease in membrane porosity, with a reduction in surface area. In addition, it led to a decrease in solution permeation rates and an improvement in salt rejection. In spite of the more pronouced reduction in porosity for GOX nanocomposite membranes, their permeation rates were higher and salt rejection lower than the CNT nanocomposite membranes. Moreover, for the CNT membranes, permeation rates decreased, with an associated increase in salt rejection, as CNT content increased. On the other hand, for the GOX nanocomposite membranes, permeation rates increased, with an associated decrease in salt rejection, as the GOX content increased. This seems to indicate the role played by the interfacial region between nanofiller and polymer matrix in membrane performance.

REFERENCES

[1] T. Mezher, H. Fath, Z. Abbas, A. Khaled. Desalination, 266, 263-273, 2011.

[2] B.M. Ganesh, A.M. Isloor, A.F. Ismail: Desalination, 313, 199-207, 2013.

[3] S. Xia, M. Ni. Journal of Membrane Science, 473, 54-62, 2015.

[4] N. El-Badawi, A.R. Ramadan, A.M.K. Esawi, M. El-Morsi. Desalination, 344, 79-85, 2014.

[5] L. Wang, X. Song, T. Wang, S. Wang, Z. Wang, C. Gao C. Applied Surface Science, 330, 118-125, 2015.

[6] P.S. Goh, A.F. Ismail, B.C. Ng. Desalination, 308, 2-14, 2013.

[7] N. Wei, X. Peng, Z. Xu Z. ACS Applied Materials & Interfaces, 6, 5877-5883, 2014.

[8] C. Gao, C.D. Vo, Y.Z. Jin, W. Li, S.P. Armes. Macromolecules, 38, 8634–8648, 2005.